ARCTIC TROPOSPHERIC WINDS FROM SATELLITE SOUNDERS

J. A. Francis, E. Hunter, C.-Z. Zou, and J. Key
NOAA/NESDIS, 1225 W. Dayton St., Madison, WI 53706

ABSTRACT

Accurate three-dimensional wind fields are essential for diagnosing a variety of important climate processes in the Arctic, such as the advection and deposition of heat and moisture, changes in circulation features, and transport of trace constituents. In light of recent studies revealing significant biases in upper-level winds over the Arctic Ocean from reanalyses, we generate new daily wind fields from over 22 years of satellite-retrieved thermal wind profiles, corrected with a recently developed mass-conservation scheme. Compared to wind measurements from rawinsondes during the Surface Heat Balance of the Arctic (SHEBA) experiment, biases in satellite-retrieved winds are near zero in the meridional direction, versus biases of over 50% for reanalyses. Errors in the zonal component are smaller than those observed in reanalysis winds in the upper troposphere, while in the lower troposphere the effects of Greenland introduce uncertainty in the mass conservation calculation. Further reduction in error may be achieved by incorporating winds retrieved from feature-tracking techniques using satellite imagers. Overall, satellite-retrieved winds are superior to reanalysis products over the data-sparse Arctic Ocean and provide increased accuracy for analyses requiring wind information.

Trends and anomalies for the 22-year record are calculated for both meridional and zonal winds at eight levels between the surface and 300 hPa. Annual mean trends are similar at varying levels, reflecting the relatively barotropic nature of the Arctic troposphere. Zonal winds are more westerly over Eurasia and the western Arctic Ocean, while westerlies have weakened over northern Canada. Combined with the corresponding pattern in meridional winds, these results suggest that the polar vortex has, on average, shifted toward Siberia. Seasonal trends show that some changes persist throughout the year while others vary in magnitude and sign. Most striking are spring patterns, which differ markedly from the other seasons. Changes in meridional winds are consistent with observed trends in melt onset date and sea ice concentration in the marginal seas. The winter NAO (North Atlantic Oscillation) index correlates moderately with meridional wind anomalies in the Atlantic sector of the Arctic Ocean: positively (0.48) in the Barents Sea and negatively (-0.59) in the Lincoln Sea. These observed trends and anomalies are expected to translate to changes in advected heat and moisture into the Arctic basin, which are likely linked to trends in sea ice extent, melt onset, cloud properties, and surface temperature.

1. Introduction

Numerous recent studies reveal a plethora of evidence that the Arctic environment has undergone rapid, perhaps unprecedented, change in the past few decades [e.g., Overland *et al*, 2003; Serreze *et al*, 2000; Overpeck *et al,* 1997]. Among these is a significant decrease in sea level pressure [Walsh *et al,* 1996], a fundamental atmospheric parameter that governs surface wind patterns, sea ice motion, and air-surface turbulent energy exchange. To understand the observed changes, as well as their roles in a variety of climate applications -- such as analyses of circulation features and disposition of advected energy, moisture, and trace constituents -- accurate upper-level wind fields are required. Over regions of the world where conventional data are sufficiently dense, the operational reanalyses fulfill this requirement with products that are generally faithful to reality. In high-latitudes, however, where observations are sparse (fewer than 5 observations per 2.5° lat-long box per month [Kistler *et al*, 2001]) the accuracy of reanalysis products in upper levels is uncertain. This is especially true over the Arctic and Southern Oceans, where rawinsonde data are typically limited to coastal stations, passing ships, temporary ice stations, and short-duration field programs.

Substantial errors in upper-level winds from two reanalysis products over the Arctic (NCEP/NCAR (National Centers for Environmental Prediction/National Center for Atmospheric Research) and the ECMWF (European Center for Medium Range Weather Forecasting) Reanalyses) were found by Francis [2002] and by Wang *et al.* [2003]. These errors have serious implications for using reanalysis wind fields for Arctic climate research, thus more accurate upper-level wind fields over the Arctic Ocean are needed. In this paper we describe a thermal-wind-based approach to produce 3D winds over the Arctic Ocean. We adapt the technique of Slonaker and Van Woert [1999], who used satellite-derived temperature profiles from the TIROS Operational Vertical Sounder (TOVS) instrument to obtain thermal winds. In modifying this method for the Arctic, we combine thermal winds with surface pressure fields and 10-meter winds from the NCEP/NCAR Reanalysis and apply the mass conservation technique of Zou and Van Woert, 2001; 2002 (hereafter ZVW1, ZVW2) to account for ageostrophic flows. We compare these fields with rawinsonde observations from the year-long Surface Heat Budget of the Arctic (SHEBA) field project [Uttal *et al,* 2002], which was conducted in the Beaufort Sea beginning in October 1997. Finally we present an analysis of 23-year trends and anomalies in zonal and meridional wind components at two representative levels. These patterns may aid in explaining observed changes in sea ice extent in regions where wind forcing is dominant, and they likely contribute to changes in advective heating, net precipitation, and cloud formation.

2. Methodology

The wind retrieval algorithm begins by obtaining temperature profiles retrieved from the TOVS instrument using the Improved Initialization Inversion ("3I") algorithm [Chédin *et al,* 1985; Scott *et al*, 1999], which includes modifications to improve accuracy over snow- and sea-ice-covered areas [Francis, 1994]. Retrieved temperatures at 9 standard levels (1000, 900, 850, 700, 600, 500, 400, 300, and 100 hPa) and the surface within 12 hours of 1200 UTC each day are averaged to form daily means, then interpolated to a 1° x 1° grid over the region north of 60°N. Gridded values are filtered zonally and meridionally to remove high-frequency noise. Layer-mean temperatures are then calculated between the standard levels listed above. The daily-mean 10-meter winds and surface pressures produced by the NCEP/NCAR Reanalysis are obtained from NCAR via ftp and interpolated to this grid. Surface pressures are used to define the layer between the surface and 1000 hPa.

Thermal winds are computed using the standard method [e.g., Wallace and Hobbs, 1977] from the thickness gradients in each layer and in the zonal and poleward directions. Thermal winds are added sequentially upward beginning with the NCEP/NCAR 10-meter u and v winds to create a first-guess wind profile. Over Greenland where TOVS profiles are not retrieved, we substitute NCEP/NCAR Reanalysis winds for levels above 700 hPa. The accuracy of reanalysis winds over Greenland is not known.

ZVW1 and ZVW2 found that thermal-wind-derived profiles improved markedly in both the general circulation structure and wind speed when a mass conservation constraint is applied both zonally and meridionally. ZVW2 developed and tested two techniques, both of which integrate the mass conservation equation (1) in a vertical column of the atmosphere:

$$\nabla \bullet \int_{p_T}^{p_s} \boldsymbol{V} \, dp = -\omega = -\frac{\partial p}{\partial t}, \qquad (1)$$

where p_s is the surface pressure, p_T is the pressure at the top of the column (assumed to be 100 hPa), and $\boldsymbol{V}$ is the horizontal wind vector. The vertical velocity is represented by ω and $\partial p/\partial t$, where $\omega = 0$ at the top of the column and $\omega = \partial p_s/\partial t$ at the surface. ZVW2 then integrate (1) around a latitude circle and along meridians to get a meridional mass flux conservation equation that contains only the meridional wind component.

Their wind retrieval approach includes two steps. The first step is to obtain a first-guess wind profile at selected tropospheric levels by adding the thermal wind derived from TOVS temperature profiles to the corresponding surface wind. The second step is to force the first-guess winds to conserve mass in a variational procedure so the winds satisfy complete dynamic constraints. Specifically, the final wind is obtained by solving a variational function in which the differences between the final wind and the first-guess wind are minimized in a least-squares sense subject to the mass conservation constraint. The meridional mass flux conservation equation is first applied across latitudinal walls to force the first-guess *v*-component wind to conserve mass. The vertically-integrated mass conservation equation is then used to infer the zonal wind. For further detail on the method and results see ZVW1, ZVW2.

In an attempt to extend this work and produce three-dimensional wind fields for the Arctic region with smaller biases and RMSEs than those from reanalysis products, we adapt the mass conservation method of ZVW2 to TOVS-derived thermal wind profiles north of 60°N. Applying their method to the Arctic is somewhat problematic, however, owing to the existence of Greenland in many of the latitude zones. This is of particular concern in the integration for the *u* wind component, as Greenland acts like a barrier below about 700 hPa and frequently generates orographically forced flows, such as katabatic winds, of its own. Having tested several methods to resolve this issue, the smallest error was obtained by linearly interpolating retrieved winds on either side of Greenland at each level below 700 hPa. Above 700 hPa we use NCEP/NCAR reanalysis winds, as we do not retrieve temperature profiles from TOVS over high elevation areas, and the flow above 700 hPa should be less affected by the orography. This issue may be revisited in the future using satellite-tracked atmospheric features to obtain upper-level winds over Greenland. For further details on the methodology used for Arctic wind retrievals, see Francis *et al.*, [in press].

3. Results

3.1 Validation

Wind fields calculated from the combination of TOVS-retrieved temperature profiles and NCEP/NCAR reanalysis 10-meter winds are validated with nearly one year of rawinsonde measurements at the SHEBA site located in the Beaufort Sea. The daily-mean TOVS winds are averaged within 100 km of the SHEBA location, then compared with daily averages of rawinsonde observations. Figure 1 presents summary statistics for both first-guess thermal wind profiles (no mass conservation) and winds corrected using the ZVW2 mass conservation scheme in which the meridional and zonal constraint is applied separately.

The results for thermal-wind-only wind retrievals (dashed lines in Fig. 1) show that, like the reanalyses, the biases in the *u*-component thermal wind profiles are positive, indicating that retrieved winds are too strong from the west. Unlike the reanalyses, however, the biases do not increase appreciably with height. The retrieval biases are about 1 m s^{-1} at the surface and are approximately constant at 3 m s^{-1} with height above 800 hPa. The biases in *v*-component thermal wind profiles also exhibit the same sign as the reanalyses but are about half the magnitude above 700 hPa. The Spearman's rank correlation coefficients are approximately 0.7 for both components (not shown), with RMSEs increasing with height from 2 m s^{-1} to about 10 m s^{-1} near the tropopause. The observed jump in RMSE from the surface to the next level above is caused by boundary layer effects and the relatively coarse vertical resolution of TOVS temperature retrievals. Particularly in the winter Arctic, strong near-surface temperature inversions and corresponding vertical wind shears are common, which are difficult to capture precisely with satellite sounders. Note that RMSEs in rawinsonde winds are estimated to be approximately 2 to 3 m s^{-1} below the jet stream level [http://www.eumetsat.de/en/dps/mpef/products/windsuse.html], thus a significant fraction of the RMSE shown in Figs. 1 and 2 may be contributed by errors in rawinsonde measurements.

The solid lines in Fig. 1 are wind retrievals with the ZVW2 mass conservation correction applied. In all but the RMSE for the zonal wind component, errors compared to rawinsondes have clearly been reduced subsequent to applying the mass conservation constraints. The error reduction for winds in the Arctic is not as substantial, however, as those achieved by ZVW2 in the Southern Ocean. We attribute this to the complicating effects of Greenland in the zonal flow as well as smaller errors in the Arctic first-guess thermal wind profiles. Biases in the TOVS-derived *u* winds have decreased 18% on average between the surface and 300 hPa, and biases in *v* are 66% lower on average owing to the mass-conservation constraint. Average RMSEs in *u* are slightly

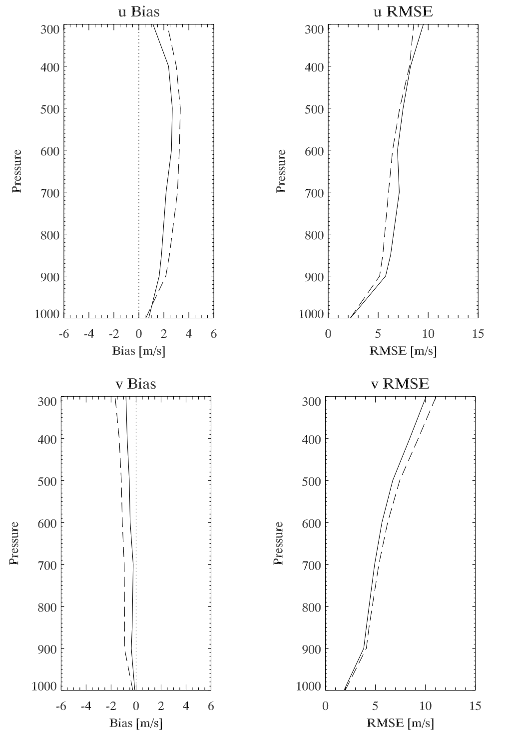

Figure 1: Error statistics for comparisons of satellite-derived wind profiles with rawinsonde measurements during SHEBA. Upper plots show zonal (*u*) winds, lower plots are meridional (*v*) winds, left are mean errors (TOVS-SHEBA) and right are root-mean-square errors. Dashed lines are thermal wind profiles with no mass conservation correction, and solid lines are retrievals with the ZVW2 mass conservation method applied.

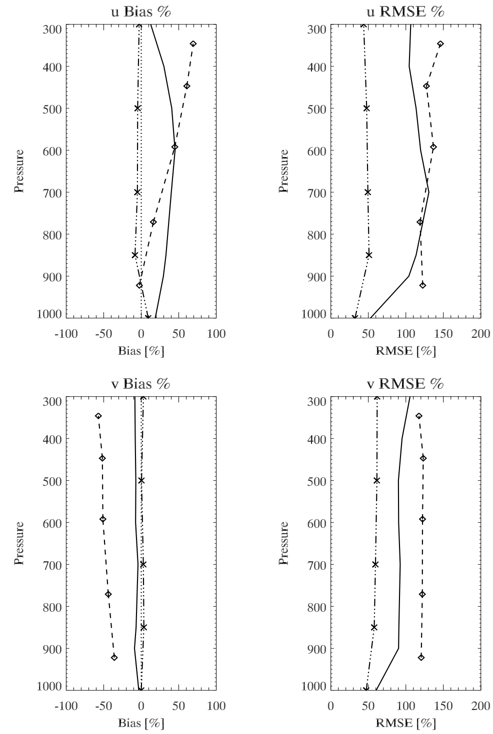

Figure 2: Comparison of error statistics for polar tropospheric winds from three sources. Dashed line is NCEP/NCAR Reanalysis versus rawinsonde data from two Arctic field programs [from Francis, 2002]; dash-dot line is for TOVS-derived winds versus rawinsonde data from Macquarie Island in the Southern Ocean [from Zou and Van Woert, 2002]; and solid line is for TOVS-derived winds versus SHEBA rawinsondes [from this study]. Biases and RMSEs have been normalized by mean *u* and *v* for each site.

higher (8%) and in *v* are slightly lower (8%). The dramatic decrease in meridional errors is encouraging for applications of wind retrievals to calculations of poleward moisture and heat advection. We also find a significant improvement in total wind speeds retrieved from TOVS compared with rawinsonde measurements. While NCEP/NCAR and ECMWF reanalyses exhibited biases whose magnitudes were over half of the actual wind speeds, the TOVS-derived biases are only about 10% of total wind speeds.

Figure 2 presents a comparison of biases and RMSEs for three sources of polar wind information: NCEP/NCAR reanalysis versus rawinsonde measurements from two Arctic field programs [from Francis, 2002]; TOVS retrievals versus rawinsonde data at Macquarie Island in the Southern Ocean [from ZVW2]; and results from this study versus rawinsonde data measured during SHEBA in the Beaufort Sea. Biases and RMSEs have been normalized by the mean absolute u and v wind speeds measured by the respective rawinsondes in an attempt to account for the effect of mean wind speed on the error statistics. Both Arctic wind products (NCEP/NCAR and this study) exhibit positive biases in the zonal component, indicating that winds are stronger from the west than rawinsonde observations. Below 500 hPa the biases in TOVS retrievals are larger than for the NCEP/NCAR Reanalysis product, and above this level the NCEP/NCAR errors are larger. We attribute this result to the effects of Greenland in the mass-conservation correction scheme, and also to the fact that the validation site for the reanalysis product is not far from coastal rawinsonde stations, whose data were ingested into the reanalysis. This is also the likely explanation for the reanalysis RMSEs being smaller than either of the TOVS retrievals. The ZVW2 biases are impressively small, especially considering that the mean zonal winds near Macquarie Island are approximately five times stronger than at either of the Arctic sites. While their RMSEs are larger than the other two sources, it is largely because of the stronger winds. In the meridional direction the two TOVS-derived wind products have very small biases, with values slightly negative in the Arctic and near zero in the Southern Ocean. The biases in the reanalysis product are relatively large and negative, indicating winds in this region are too strong from the north. These results further support the use of TOVS-derived wind fields, especially the meridional component, for calculations of energy and moisture transport.

3.2 Trends

Nearly twenty-three years (mid-1979 to 2001) of TOVS-derived upper-level winds have been used to analyze temporal changes over the Arctic basin. At each latitude/longitude grid point we calculate the least-squares linear fit to the *u* and *v* wind components, the slope of which is plotted if its significance exceeds the 90% confidence level. Trends are calculated at one-degree lat/lon resolution for the total troposphere below 300 hPa and for each of 8 levels between the surface and 300 hPa over the entire year and for each season. Note that because thermal winds are derived from horizontal temperature *gradients*, any errors resulting from intra- or inter-satellite biases will subtract out, thus analyses of trends and variability are unaffected.

The general wind climatology derived from TOVS-retrieved winds is described for six representative regions of the Arctic (defined in Table 1). In most areas, the zonal winds at 300 hPa are predominantly positive, as would be expected near the jet-stream level. Negative (easterly) excursions occur every few years in the Lincoln and Laptev Seas, however, caused by splitting of the polar vortex with a lobe centered south of the regions. Meridional winds are more variable among the six areas. Barents Sea winds are predominantly from the north, as the area is usually located in the ridge downstream from the Icelandic low. Similarly the Laptev Sea region generally experiences flow from the south owing to the tendency for a trough just west of the area. At 700 hPa winds are generally weaker, while predominant tendencies in direction are similar.

Table 1: Regions defined for time series and anomaly analysis.

Region Name	Latitude bounds	Longitude bounds
Barents Sea	73 to 78°N	30 to 60°E
Laptev Sea	73 to 78°N	110 to 140°E
E. Siberian Sea	73 to 78°N	150 to 180°E
Beaufort Sea	73 to 78°N	195 to 225°E
Lincoln Sea	78 to 88°N	240 to 270°E
North Pole	85 to 90°N	0 to 360°

Figure 2 presents 23-year annual trends (m s^{-1} $decade^{-1}$) for the zonal and meridional wind components for the total troposphere, as well as for two representative levels: 300 and 700 hPa. We have compared TOVS-derived trends to those computed from NCEP/NCAR Reanalysis winds over land areas where rawinsonde data are relatively dense, and the patterns agree well (not shown). Large areas of significant changes in both *u* and *v* are evident in Fig. 2. Our discussion will focus primarily on Arctic Ocean areas where TOVS provides new information.

Zonal winds in much of the eastern Arctic Ocean have become less westerly (from the west) at all levels, while trends in the western Arctic are less cohesive and generally positive. These features, together with positive trends over the northern Eurasian continent, suggest that the polar vortex has strengthened and/or shifted toward Siberia. The pattern in meridional winds is consistent with this explanation, as trends are generally positive near the dateline and negative over the Barents/Kara Seas. A general tendency toward positive meridional trends over the eastern half of Eurasia suggest increased warm advection, which is consistent with observed changes in surface temperature [e.g., Rigor *et al*, 2000]. Patterns are similar for the total troposphere, 300, and 700 hPa levels, indicating that the atmosphere is, on average, relatively barotropic. In the lower troposphere (represented by the plot for 700 hPa), the trend patterns are consistent with the shift in the Beaufort Gyre from the 1980s to the 1990s identified by Rigor *et al.* [2002] using satellite-monitored motions of buoys on the pack ice during winter. They found that during the 1990s the transport shifted eastward in the Barents/Kara Seas, increased northward in the Siberian Sea, and was stronger southward through the Fram Strait as compared to the previous decade.

A comparison of the patterns among the seasons (not shown) reveals some persistent characteristics as well as some seasonally varying features. The zonal component (*u*) exhibits a moderate degree of similarity through the seasons. The summer season exhibits only small trend values. The eastern Arctic Ocean is characterized by decreasing westerly winds through most of the year, while winds are more westerly in the Green-

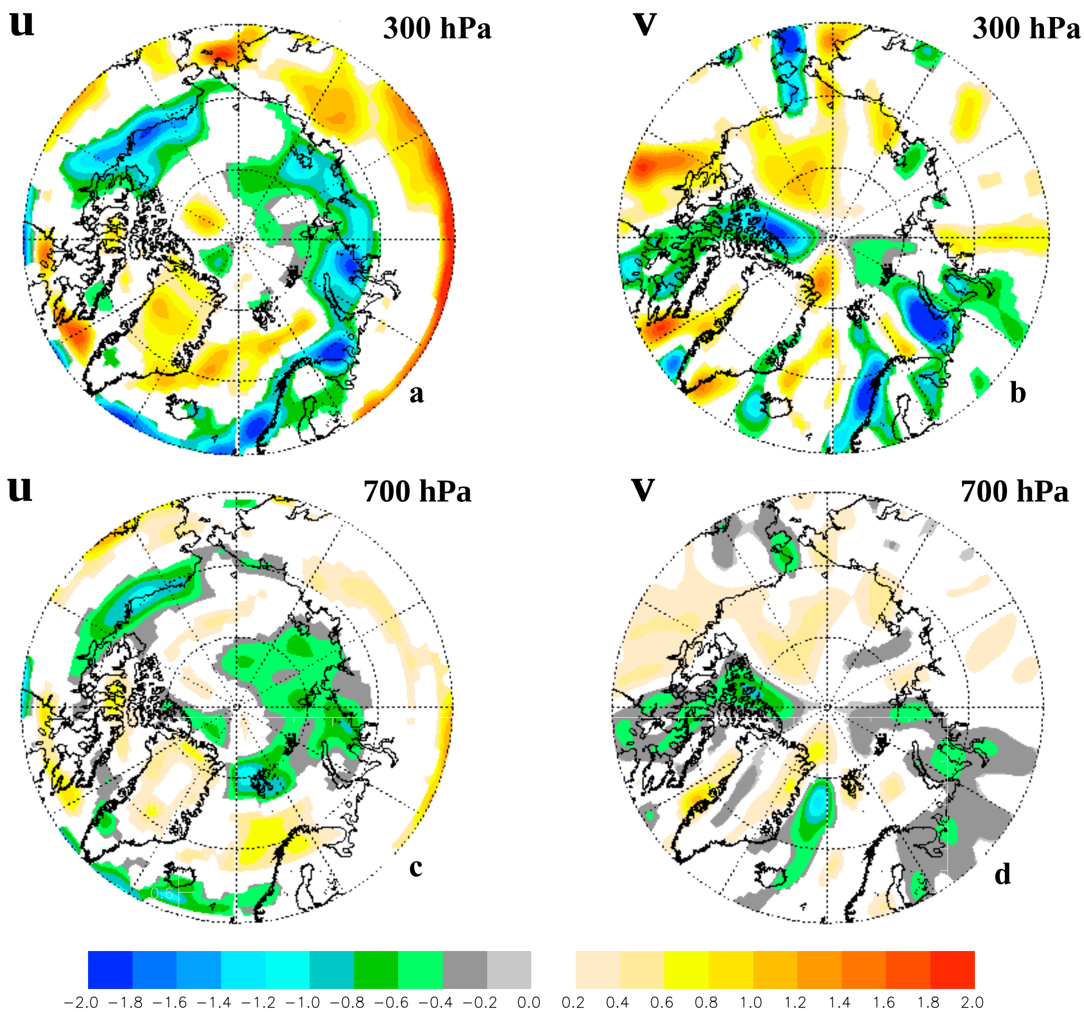

Figure 2: 23-year trends (1979 to 2001) in zonal (left) and meridional (right) wind derived from TOVS temperature profiles over the entire year. Top plots are for the 300 hPa level, and bottom are for the 700 hPa level. Units are m s^{-1} $decade^{-1}$.

land Sea area during autumn and winter. An area with consistent negative trends appears along the coasts of northwest Canada and northern Alaska. Confidence in this feature is weaker, however, as orographic effects likely play a role in low level winds, and trends in winds from the NCEP/NCAR reanalysis show less consistency with TOVS-derived patterns. In general, the Arctic Ocean is dominated by negative trends in autumn and winter, indicating a weakening or perhaps shifting of the polar vortex.

In trend patterns for the meridional component (*v*), spring stands out as having a different pattern from the other seasons, with a strong increase in southerly winds on the Pacific side of the Arctic, which is consistent with the distinct spring warming trend in the lower troposphere diagnosed by Overland *et al.* [2002] from TOVS Path-P retrievals and NCEP/NCAR Reanalyses. Spring is also characterized by strong positive trends in the Barents/Kara Seas as well as negative trends over the GIN (Greenland-Iceland-Norway) Seas. Correlations between spring trends and values for other seasons as well as the annual trend are consistently weak for both *u* and *v* components, suggesting that changes in the spring circulation may result from forcings or interactions that are different from the rest of the year. One candidate is a change in surface melt onset, which corresponds to a sharp decrease in surface albedo and surface-absorbed solar radiation. Satellite-derived estimates of melt-onset date by Belchansky *et al.* [2003] indicate that melting occurred 10 to 20 days earlier during the 1990s versus the 1980s in the Pacific sector of the Arctic where TOVS-derived meridional winds exhibit significant positive trends in spring. Negative trends in *v* winds over the Laptev Sea in winter and spring coincide with later melt-onset dates in their analysis. A definite causal relationship cannot be implicated at this time, but the correspondence is suggestive of a process responsible for the distinctive patterns in spring trends.

The summer/autumn patterns in the *v* component display several common features, as well, particularly in the Barents/Kara sector, where a large area of negative trend (more northerly wind) appears. Southerly trends in the Siberian Sea in spring and autumn implicate a possible mechanism for dynamic sea ice removal in an area where decreasing sea ice concentrations have been observed [e.g., Comiso, 2000; Parkinson and Cavalieri, 2002]. In spring the Barents Sea exhibits positive trends, coinciding with the break-up of annual ice, and consequently this area may be more susceptible to dynamic ice removal than in other seasons. Meridional atmospheric temperature gradients are large in late spring as the land warms before the ocean, thus positive trends in *v* likely translate to stronger poleward heat advection. Northerly trends in the Lincoln Sea (north of the Canadian Archipelago) may contribute to observed increases in ice concentrations in this area, while the northerly trends in the western GIN Seas, especially in spring, likely contribute to increased ice advection and observed concentration decreases in this area.

Additional details on seasonal trends, analyses of time series and anomalies, as well as relationships with the NAO can be obtained from Francis et al., [2004].

4. Conclusions

Recent studies have revealed significant changes in the Arctic circulation in the past few decades, but also that upper-level winds over the Arctic Ocean from operational reanalyses exhibit large biases relative to rawinsonde measurements. Reliable wind fields are essential for accurate calculations of atmospheric transport of heat, moisture, and pollutants, as well as for understanding relationships among changing atmospheric and surface parameters. In an attempt to improve upon this situation, a new 23-year (1979 – 2001) product of three-dimensional wind fields in the Arctic troposphere has been generated from satellite-derived temperature soundings.

Trends and anomalies for the 23-year record are calculated from the satellite-derived wind fields. Annual-mean trends in both *u* and *v* components at varying levels are well correlated, suggesting that the Arctic atmosphere is nearly barotropic. On annual average the zonal winds exhibit positive trends (more westerly) over most of Eurasia between 60°N and 70°N, while winds are weaker from the west over the eastern Arctic Ocean and northwestern Canada/Alaska. A corresponding pattern appears in the meridional trends, which suggests that the polar vortex has shifted toward Siberia. Increased offshore winds in the E. Siberian Sea, as well as in the Barents Sea during spring and summer, may aid in explaining observed decreases in sea ice extent in those areas.

A separation of trends into the four seasons reveals that many features persist through the year, while some vary in strength and sign. Spring patterns in meridional trends appear to correspond with observed changes in melt onset date, which may implicate a spring-only interaction responsible for the seasonal differentiation in trends. Dynamic forcing of sea ice may be stronger in spring, when first-year ice is breaking up and the boundary layer stratification is weakening, implying that trends in spring winds may have a stronger relationship with observed changes in sea ice concentration. Indeed the spring *v*-component trends appear to agree well with sea ice change: increased southerly flow at 700 hPa corresponds with decreased ice concentrations in the E. Siberian and Barents Seas, while increased northerly flow occurs where ice has increased north of the Canadian Archipelago and where decreased ice cover is observed in the western GIN Seas. Increased advective heating may also play a role where stronger southerly flow interacts with steep horizontal temperature gradients in spring.

In summary, a new three-dimensional wind product has been generated from 23 years of satellite temperature retrievals over the Arctic Ocean. Accuracies appear to surpass winds from reanalyses, particularly in the poleward direction, which will increase confidence in studies of Arctic atmospheric circulation features. In particular, improved wind fields will increase the accuracy of calculated heat and moisture transport into and within the Arctic from lower latitudes, which constitutes the single largest source of energy for the Arctic climate system.

Acknowledgements. The authors are very grateful to the anonymous reviewer and to the editor for their valuable and constructive suggestions. This work was supported by grants OPP-0105461 and OPP-0240791 from NSF and UAF02-0032 from NOAA/University of Alaska. The contents of this paper are solely the opinions of the authors and do not constitute a statement of policy, decision, or position on behalf of NOAA or the U.S. Government.

5. REFERENCES

Belchansky, G. I., D. C. Douglas, and N. G. Platonov, 2003: Duration of the Arctic sea ice melt season: Regional and interannual variability, 1979-2001. *J. Clim*, in press.

Chédin, A., N.A. Scott, C. Wahiche, and P. Moulinier, 1985: The Improved Initialization Inversion method: A high resolution physical method for temperature retrievals from satellites of the TIROS-N series, *J. Clim. Appl. Meteorol., 24,* 128-143.

Comiso, J.C. [2000]. A rapidly declining Arctic perennial ice cover. Geophys. Res. Lett., 29, 1956, doi:10.1029/2002GL015650.

Francis, J.A., E. Hunter, and C.-Z. Zou, 2004: Arctic Tropospheric Winds Derived from TOVS Satellite Retrievals, *J. Clim.*, in press.

Francis, J.A., 2002: Validation of reanalysis upper-level winds in the Arctic with independent rawinsonde data, *Geophys. Res. Lett., 29,* 10.1029/2001GL014578.

Francis, J.A., 1994: Improvements to TOVS retrievals over sea ice and applications to estimating Arctic energy fluxes, *J. Geophys. Res., 99,* 10,395-10,408.

Kistler, R. and 12 co-authors, 2001: The NCEP/NCAR 50-year reanalysis: monthly means CD-ROM and documentation, *Bull. Am. Meteor. Soc., 82*, 247-267.

Overland, J.E., M. C. Spillane, and N. N. Soreide, 2003: Integrated analysis of physical and biological pan0Arctic change. *Climatic Change,* in press.

Overland, J.E., M. Wang, and N.A. Bond, 2002: Recent temperature changes in the western Arctic during spring. *J. Clim., 15,* 1702-1716.

Overpeck, J. T. and 17 others, 1997: Arctic environmental change of the last four centuries. *Science, 278,* 1251-1256.

Parkinson, C.L., and D.J. Cavalieri. 2002. A 21 year record of arctic sea-ice extents and their regional, seasonal and monthly variability and trends. Annals of Glaciology 34: 441-446.

Rigor, I.G., R.L. Colony, and S. Martin, 2000: Variations in surface air temperature in the Arctic from 1979-1997. *J. Clim., 13,* 896-914.

Rigor, I. G., J.M. Wallace, and R. L. Colony, 2002: On the Response of Sea Ice to the Arctic Oscillation, *J. Climate, 15(18)*, 2546-2663.

Scott, N.A., A. Chedin, R. Armante, J. Francis, C. Stubenrauch, J.-P. Chaboureau, F. Chevallier, C. Claud, and F. Cheruy, 1999: Characteristics of the TOVS Pathfinder Path-B dataset. *Bull. Am. Meteor. Soc., 80,* 2679-2701.

Serreze, M. C., J. E. Walsh, F. S. Chapin III, T. Osterkamp, M. Dyurgerov, W. Oechel, J. Morison, T. Zhang and R. G. Barry, 2000: Observational evidence of recent change in the northern high-latitude environment. *Climatic Change, 46,* 159-207.

Slonaker, R.L. and M.L. Van Woert, 1999: Atmospheric moisture transport across the Southern Ocean via satellite observations. *J. Geophys. Res., 104*, 9229-49.

Susskind, J., P. Piriano, L. Rokke, L. Iredell, and A. Mehta, 1997: Characteristics of the TOVS Path A data set. *Bull. Amer. Meteorol. Soc., 78,* 1449-72.

Uttal, T. and 26 co-authors, 2002: The Surface Heat Budget of the Arctic Ocean, *Bull. Am. Meteor. Soc., 83,* 255-276.

Wallace, J.M. and P. V. Hobbs, 1977: *Atmospheric Science: An Introductory Survey.* Academic Press, 467 pp.

Walsh, J. E., W. L. Chapman and T. L. Shy, 1996: Recent decrease of sea level pressure in the central Arctic. *J. Climate, 9.* 480-486.

Wang, S.-H., J.A. Francis, and D.H. Bromwich, 2003: Evaluation of the NCEP/NCAR and ECMWF 15-year reanalyses over the data-sparse Arctic Ocean. *Proceedings from the 7th Conference on Polar Meteorology and Oceanography*, Am. Meteor. Soc., 12-16 May 2003, Hyannis, MA.

Zou, C.-Z. and M. L. Van Woert, 2001: The role of conservation of mass in the satellite-derived poleward moisture transport over the Southern Oceans. *J. Climate, 14*, 997-1016.

Zou, C.-Z. and M. L. Van Woert, 2002: Atmospheric wind retrievals from satellite soundings over the middle and high latitude oceans, *Mon. Wea. Rev., 130,* 1771-1791.